Phys. Chem. Glasses: Eur. J. Glass Sci. Technol. B, October 2015, **56** (5), 177–182

A ^{10}B NMR study of trigonal and tetrahedral borons in ring structured borate glasses and crystals

Miles Faaborg,[1] Kyle Goranson,[1] Nathan Barnes,[1] Evan Troendle,[1] Rachel Rice,[2] Michael Chace,[1] Luke Montgomery,[1] Andrew Koehler,[1] Zachary Lindeberg,[2] Diane Holland,[3] Mark E. Smith,[3,4] Mario Affatigato,[1] Steve Singleton[1] & Steve Feller[1]

[1] *Physics Department, Coe College, Cedar Rapids, IA 52402, USA*
[2] *Mathematics and Physics Departments, Simpson College, Indianola, IA 50125, USA*
[3] *Department of Physics, University of Warwick, Coventry, CV4 7AL, UK*
[4] *Vice-Chancellor's Office, University House, Lancaster University, Lancaster, LA14YW, UK*

Manuscript received 1 November 2014
Revised version received 18 December 2014
Accepted 6 July 2015

We used ^{10}B NMR and our previously developed Spectrafit automatic fitting program to determine the best values of the quadrupole parameters of both trigonal and tetrahedral borons in intermediate range structures. Each boron site was characterised by the quadrupole coupling constant, C_Q, the asymmetry parameter, η, and their respective standard deviations, σ_{C_Q} and σ_η, assumed Gaussian. The results lead us to believe that η is especially sensitive to the length scale of the intermediate range order.

1. Introduction

Nuclear magnetic resonance (NMR) spectroscopy is a widely used technique for studying short range order in glass. In some cases, nuclei that have particularly strong interactions with bonding electrons may also be used to investigate intermediate range order (IRO) on a scale of 5 to 10 Å. Several NMR techniques may be used for this purpose, including the homo- and heteronuclear dipolar interactions[(1)] and the quadrupole interaction; this paper will focus on the latter, and in particular on the ^{10}B quadrupole interaction. ^{10}B is an appropriate isotope because of its strong quadrupole interaction and spin of three, which gives its powder patterns a high degree of detail, sensitive to both the quadrupole coupling constant, C_Q, and to the asymmetry parameter, η, and their distributions. Unfortunately, a full ^{10}B NMR spectrum from trigonal borons covers a wide frequency range, often exceeding 1·4 MHz, needing approximately one to two weeks of runtime to improve the signal-to-noise ratio to an acceptable level. These difficulties make ^{10}B NMR an unpopular choice in the field of glass science, particularly in industry; however, the detail available in a ^{10}B NMR spectrum provides an opportunity to reveal structural information at the IRO level.

Recently, we reported on an automated fitting procedure called *SpectraFit*[(2)] that we developed to determine both the average C_Q and η values present in borates as well as the standard deviations of those values, denoted by σ_{C_Q} and σ_η, respectively. In this work we have extended the fitting routine to allow rapid and precise fitting of two overlapping boron sites by adding a multimillion spectra library, in which C_Q and η were varied systematically in small steps. In addition, we developed algorithms to increase the efficiency of the searches, allowing rapid comparison of distributed powder patterns to experimental data.

We used the latest version of *SpectraFit* to examine ^{10}B NMR spectra from borates that exhibit two distinctive environments. We examined crystalline and vitreous cesium triborate ($Cs_2O.3B_2O_3$) composed of six-membered rings with two trigonal sites and one tetrahedral site, see Figure 1, and obtained two sets of quadrupole parameters from the trigonal and tetrahedral borons from each sample. This procedure was repeated for vitreous cesium diborate ($Cs_2O.2B_2O_3$) of a known IRO, different from that of cesium triborate,

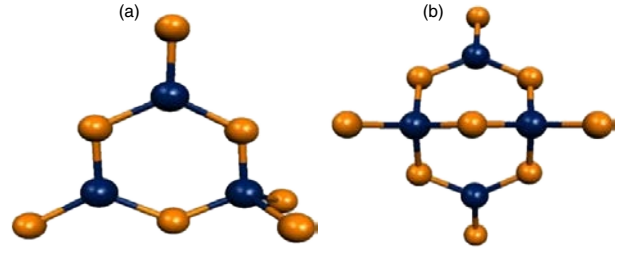

Figure 1. Intermediate borate ring structures: (a) triborate and (b) diborate (Colour available online)

* Corresponding author. Email SFELLER@coe.edu
Original version presented at VIII Int. Conf. on Borate Glasses, Crystals and Melts, Pardubice, Czech Republic, 30 June–2 July 2014
DOI: 10.13036/17533562.56.5.177

see Figure 1. In addition, we examined glassy cesium enneaborate ($Cs_2O.9B_2O_3$), a combination of boroxol and triborate rings. The quadrupole parameters from the trigonal borons were then compared to trigonal sites in glassy boron oxide and crystalline lithium orthoborate ($3Li_2O.B_2O_3$). The quadrupole parameters of the triborate and diborate tetrahedral borons were also determined.

2. Procedures

2.1 ^{10}B NMR

The pulsed NMR experiments were done statically at a central magnetic field of 7·0 T, corresponding to a Larmor frequency of 32·239 MHz, with a standard 90°–180° pulse echo, τ=3 ms, and 10–30 s pulse delay. To acquire such a wide spectrum, the magnetic field was varied by a field step unit[3] (a separate magnet was used to vary the main superconducting field). The final powder pattern is the sum of the spectra at each field. We found that about 25 steps were needed to avoid artefacts in the spectrum, and 1500 to 2500 acquisitions were needed at each magnetic field strength to yield an acceptable signal-to-noise ratio.

2.2 Sample preparation

Samples for NMR included fast, medium, and slow cooled vitreous boron oxide (B_2O_3), vitreous cesium enneaborate ($Cs_2O.9B_2O_3$), crystalline and vitreous cesium triborate ($Cs_2O.3B_2O_3$), and vitreous cesium diborate ($Cs_2O.2B_2O_3$), as well as crystalline lithium orthoborate ($3Li_2O.B_2O_3$). The samples were produced from boric acid enriched to ≥99% ^{10}B, provided by Eagle Picher, Sigma Aldrich, and Cambridge Isotopes. The samples were melted in platinum crucibles at 1000°C for 30 min. The fast cooled boron oxide was rapidly quenched using a roller quencher; the medium cooled boron oxide was prepared as droplets on a metal plate; and the slow cooled B_2O_3 glass was formed over the course of five days in a furnace contained in a nitrogen glove box to eliminate possible effects from the hygroscopicity of boron oxide. The samples of glassy cesium enneaborate, cesium triborate, and cesium diborate were prepared by mixing stoichiometric amounts of cesium carbonate and ^{10}B enriched boric acid and melting at 1000°C for 20–25 min. Weight loss was measured to confirm each of the binary glassy compositions. These samples were quenched using metal plates. Crystalline lithium orthoborate and cesium triborate were formed from ^{10}B-enriched boric acid and either lithium or cesium carbonate, melted at 1000°C, and slowly cooled in the crucible to room temperature. X-ray diffraction confirmed the sole presence of the orthoborate and triborate crystals.

Table 1. ^{10}B Quadrupole parameters for boron oxide and lithium orthoborate

Sample	C_Q *(MHz)* ±0·01 MHz	σ_{C_Q} *(MHz)* ±0·01 MHz	η ±0·01	σ_η ±0·01
Crystalline lithium orthoborate, $3Li_2O.B_2O_3$	Trigonal boron 5·55	0·11	0·06	0·00
Slow cooled (10^{-3} °C/s) glassy B_2O_3	Trigonal boron 5·42	0·26	0·10	0·02
Medium cooled (10^3 °C/s) glassy B_2O_3	Trigonal boron 5·42	0·16	0·13	0·06
Fast cooled (10^5 °C/s) glassy B_2O_3	Trigonal boron 5·40	0·26	0·12	0·06

2.3 Simulation of ^{10}B NMR spectra and boroxol ring structures

2.3.1 Simulation of ^{10}B NMR spectra

The powder pattern from quadrupole NMR does not follow a simple analytical mathematical form,[4] but its shape can be modelled theoretically using four variables to simulate the spectra: C_Q, η, σ_η, and σ_{C_Q}. Finding simulated spectra that best match the experimentally produced NMR powder patterns is computationally expensive, but once found they provide insight into the longer range structures of glassy and crystalline borate materials.

Spectrafit[2] was based on the program *QuadFit*, developed by T. F. Kemp,[5] that produced distributed powder patterns that could then be visually compared to the experimental spectra. *Spectrafit*, a program initially developed by Khristenko *et al*,[2] implemented the ability to compute how closely theoretical and experimental spectra agree, based on a calculated normalised residuals per point (NRP) value. Further details of the operation of that program are given in the paper by Khristenko.[2] The differences between the initial *Spectrafit* and the version of *Spectrafit* modified for use for in this research are noteworthy. We created a library of spectra generated by varying the four primary variables (C_Q, σ_{C_Q}, η, and σ_η) across a large range of practical values at relatively small step sizes. The result was a catalogue of possible spectra, which were quickly and automatically matched to the experimental data to find the best fit. For this research, the library of spectra was filled in at high resolution, changing each variable in steps of 0·01–0·025 MHz for C_Q and σ_{C_Q} and 0·01–0·025 for η and σ_η. In addition, the current procedure was changed to only fit spectra based on the range of the NMR powder pattern that included features from complete $m \rightarrow m-1$ transitions; as noted earlier, ^{10}B NMR requires an extraordinarily wide range of frequencies, and as a result, the ends of the experimentally produced spectra do not always include all possible features in the theoretical powder patterns of ^{10}B. Also, a version of the program was modified

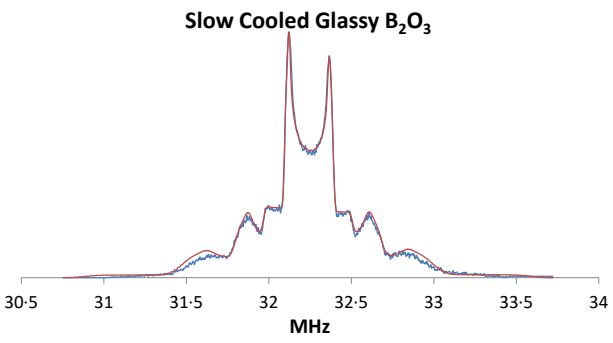

Figure 2. ^{10}B NMR spectrum from slowly cooled glassy boron oxide with the best fit spectrum superimposed in red (Colour available online)

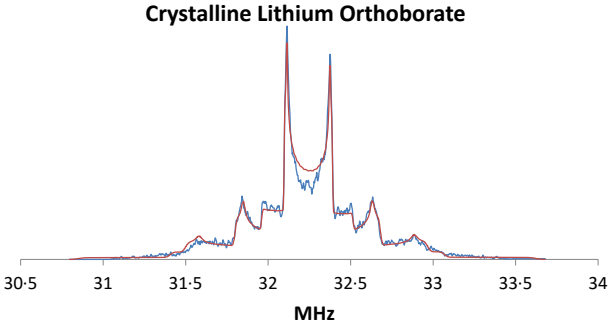

Figure 3. ^{10}B NMR spectrum from crystalline lithium orthoborate with the best fit spectrum superimposed in red (Colour available online)

to be multithreaded, so that multiple processors worked on multiple sections of the database at once. The improved resolution provided by the new library of spectra, as well as the improved fitting method, yielded simulated spectra with lower NRPs (average of 0·00393 with a standard deviation of 0·00102) and therefore stronger agreement with the experimentally generated spectra than in our earlier work.

2.3.2 Simulation of boroxol ring structures

Vitreous B_2O_3 fragments were modelled using *ab initio* methods employing the program Gaussian.[6] Fragments contained 40–80 atoms and the total number of borons in all seven fragments was 152. The fragments were constructed such that 75–80% of the boron nuclei were in rings, with an average of 77%, an arrangement that reflects the proportions of borons in rings observed in earlier reports.[7–15] Open valences on oxygen atoms were completed with hydrogen atoms, if necessary. Geometry optimisations and NMR electric field gradient tensor calculations were performed with the DFT-B3LYP/6-31G(d) model chemistry. The resulting tensors were used to calculate central values of η and C_Q, and their respective standard deviations σ_{C_Q} and σ_η, from the ensemble of borons used. All borons connected to hydroxyl groups were removed from the simulations.

3. Results

3.1 ^{10}B NMR spectra and simulations

Figures 2 to 7 show the experimental ^{10}B NMR spectra together with the simulated spectra acquired by minimising the NRPs obtained from *Spectrafit*, resulting in the quadrupole parameters given in Tables 1 and 2.

3.2 Computational models for glassy boron oxide

The calculated quadrupole parameters were obtained by minimising energy and hence optimising geometry for a variety of boron oxide fragments. The quadrupole parameters were determined by averaging over seven of these fragments (Table 3) containing 152 borons.

4. Discussion

We compare the present resultsfrom glassy boron oxide with literature values from ^{11}B NMR and NQR

Table 2. ^{10}B Quadrupole parameters for a variety of cesium borates

Sample	*C_Q (MHz) ±0·01 MHz (Trigonal boron) ±0·025 MHz (Tetrahedral boron)*	*σ_{C_Q} (MHz) ±0·01 MHz (Trigonal boron) ±0·025 MHz (Tetrahedral boron)*	*η ±0·01 (Trigonal boron) ±0·025 (Tetrahedral boron)*	*σ_η ±0·01 (Trigonal boron) ±0·025 (Tetrahedral boron)*
Cesium enneaborate glass, $Cs_2O.9B_2O_3$	Trigonal 5·38	0·31	0·16	0·09
	Tetrahedral 1·375	0·525	0·90	0·00
Cesium triborate glass, $Cs_2O.3B_2O_3$	Trigonal 5·54	0·44	0·24	0·13
	Tetrahedral 0·80	0·275	0·80	0·00
Cesium triborate crystal, $Cs_2O.3B_2O_3$	Trigonal 5·34	0·38	0·24	0·02
	Tetrahedral 0·38	0·08	0·58	0·25
Cesium diborate glass, $Cs_2O.2B_2O_3$	Trigonal 5·37	0·49	0·25	0·11
	Tetrahedral 1·25	0·525	0·125	0·075

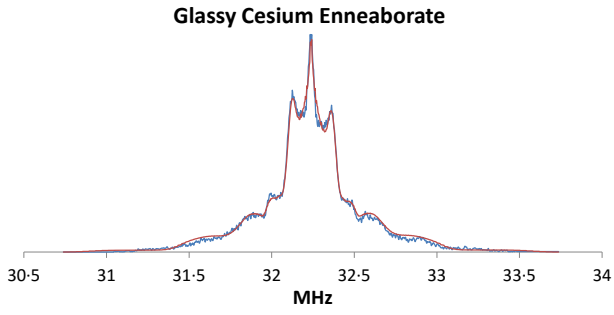

Figure 4. ^{10}B NMR spectrum from glassy cesium enneaborate with best fit spectrum superimposed in red (Colour available online)

by tabulating results for C_Q and η and for the quadrupole product, P_Q given by

$$P_Q=C_Q(1+\eta^2/3)^{0.5} \quad (1)$$

Using the ratio of the quadrupole moments of ^{10}B and ^{11}B we can find $C_Q(^{11}B)$ from $C_Q(^{10}B)$:

$$C_Q\left(^{11}B\right)=\frac{Q^{^{11}B}}{Q^{^{10}B}}C_Q\left(^{10}B\right)=\frac{1}{2{\cdot}084}C_Q\left(^{10}B\right) \quad (2)$$

Table 4 gives the comparison of the present results to those from a variety of other NMR and NQR measurements.[9,10,13,15]

The three differently cooled boron oxide glasses each contain trigonal borons with bridging oxygens (BOs) whereas crystalline lithium orthoborate contains isolated boron–oxygen triangles with all non-bridging oxygens (NBOs). The asymmetry parameter for boron oxide is larger (0·12 on average) compared to that for lithium orthoborate (0·06), presumably due to the two kinds of oxygen (in-ring and non-ring) in B_2O_3. The in-ring oxygens are bonded to two in-ring borons and the non-ring oxygens are each bonded to one in-ring boron and one non-ring boron. This arrangement contrasts with the highly symmetric non-bridging oxygens in crystalline lithium orthoborate.

Overall, the values of η for trigonal borons show a systematic increase as the number of tetrahedral borons bonded through oxygens to trigonal borons increases (Table 5). The increasing number of trigonal–tetrahedral connections increasingly breaks the cylindrical symmetry of the trigonal borons. As a result it

Table 3. Mean and standard deviation (σ) values for the asymmetry parameter and the quadrupole coupling constant of glassy B_2O_3 fragments compared with experimental results from boron oxide glass

η C_Q (MHz)	Basis	Set#	Fragments*	Mean σ	Mean σ
6-31G(d)	7	0·148	0·062	5·498	0·384
Experimental averages from boron oxide glasses		0·12±0·01	0·05±0·01	5·41±0·01	0·22±0·01

with a DFT-B3LYP used for geometrical optimisation and the resulting NMR parameters
*Boron fragments range in size from 15 to 30 borons with an average of 77% of the borons in boroxol rings

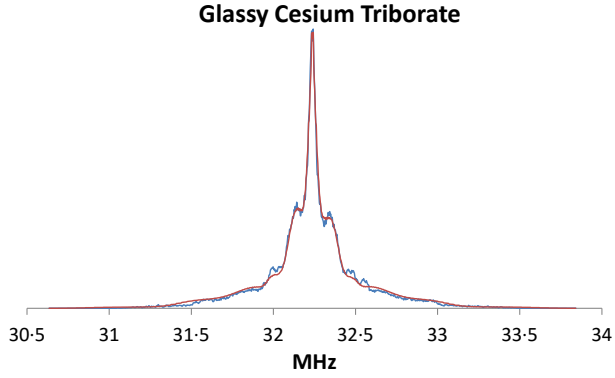

Figure 5. ^{10}B NMR spectrum from glassy cesium triborate with best fit spectrum superimposed in red (Colour available online)

appears that η is especially sensitive to the particular ring structure the trigonal borons are in.

In Table 2 we show a comparison of the quadrupole parameters from both vitreous and crystalline cesium triborate. The values for η from the trigonal borons from the two samples are both 0·24 indicating that the intermediate range order is similar between the crystal and the glass. As expected the distribution parameters (σ_{C_Q} and σ_η) are smaller for the crystal than for the glass.

The quadrupole coupling constant, C_Q, does not seem to correlate with intermediate range structure.

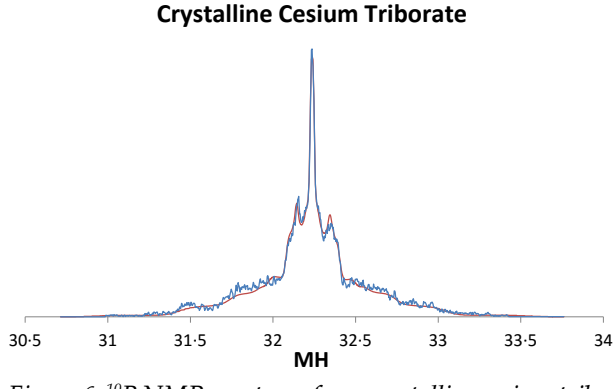

Figure 6. ^{10}B NMR spectrum from crystalline cesium triborate with best fit spectrum superimposed in red (Colour available online)

Table 4. Comparison of the present quadrupole parameter results from glassy boron oxide with those from ^{11}B NMR and NQR

Results from	Method	C_Q (MHz)	η	P_Q (MHz)
Present work	^{10}B pulsed NMR	2·60	0·13	2·61
Jellison, Panek, & Bray[9]	^{10}B wideline NMR	2·64	0·12	2·65
Hung *et al*[16]	^{11}B DOR NMR at 20 T			2·67 (Ring) 2·61 (Non-ring)
Kroeker, Neuhoff & Stebbins[17]	^{11}B MAS NMR	2·68	0·15	2·69
Gravina, Bray & Peterson[15]	^{11}B NQR			2·71 (Ring) 2·61 (Non-ring)
Hwang *et al*[13]	^{11}B MAS NMR and MQMAS NMR	2·68 2·60 (Non-ring)	0·16 0·19	2·69 (Ring) 2·62 (Non-ring)

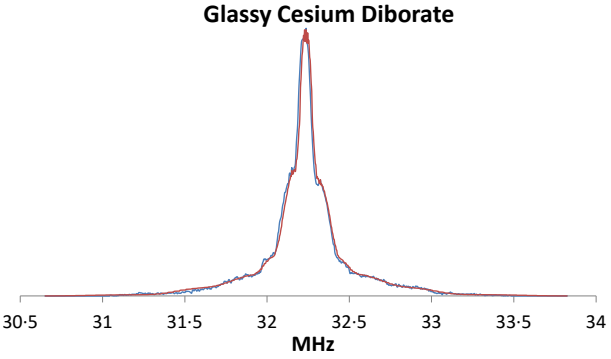

Figure 7. [10]B NMR spectrum from glassy cesium diborate with best fit spectrum superimposed in red (Colour available online)

We found precise values of C_Q for trigonal borons (Tables 1 and 2) spanning a small range from 5·34 MHz (2·56 MHz, [11]B) for crystalline $Cs_2O.3B_2O_3$, to 5·55 MHz (2·66 MHz for [11]B) for crystalline $3Li_2O.B_2O_3$; the latter value agrees reasonably well with an earlier result, 2·76 MHz, obtained using [11]B NMR.[(11)] The values of C_Q for the tetrahedral borons are considerably smaller than those for trigonal borons, ranging from 0·80 to 1·375 MHz with no clear pattern.

The standard deviations of η and C_Q show trends. The fits for glasses containing both trigonal and tetrahedral borons display a consistently larger σ_η for the trigonal borons (0·09 to 0·13, Table 2) than the fits for glasses containing only trigonal borons (0·02 to 0·06, Table 1), possibly due to increasing disorder caused by the added presence of tetrahedral borons. Similarly, σ_{C_Q} for trigonal borons is also larger for glasses with both types of sites (0·31 to 0·49 MHz, Table 2), compared with glasses with only trigonal borons (0·11 to 0·26 MHz).

The simulated boron fragments yielded quadrupole parameters comparable to the experimental parameters for boron oxide (Table 3).

5. Conclusions

We used an updated version of the program Spectrafit to determine accurate [10]B quadrupole parameters from a series of glasses and crystals, containing either trigonal and tetrahedral boron sites, or solely trigonal boron sites. The asymmetry parameter for the trigonal borons is especially sensitive to the intermediate range order of the boron rings. The quadrupole coupling constant was found to be close to 5·5 MHz for the trigonal borons without apparent pattern. It was found that the distributions of the quadrupole parameters of the trigonal borons were sensitive to the symmetry of these sites. The quadrupole coupling constants for the tetrahedral borons were about 4–5 times smaller than those for the trigonal borons. No apparent patterns were found within the parameter set for the tetrahedral borons.

Acknowledgements

We acknowledge the National Science Foundation of the United States under grants numbered NSF-DMR 1407404, NSF-DMR 1262325, NSF-REU 1358968, and NSF-REU 1004860. Mrs Janice Faaborg is thanked for help in editing the paper.

References

1. There are many references to studies that employ this technique. Three representative reference are: Ratai, E., Chan, J. C. C. & Eckert, H. *Phys. Chem. Chem. Phys.*, 2002, **4**, 3198. Epping, J. D., Stroijek, W. & Eckert, H. *Phys. Chem. Chem. Phys.*, 2005, **7**, 2384. Chen, B., Werner-Zwanziger, U., Nascimento, M. L. F., Ghussn, L., Zanotto, E. D. & Zwangziger, J. W. *J. Phys. Chem. C*, 2009, **113**, 20725.
2. Khristenko, V., Tholen, K., Barnes, N., Troendle, E., Crist, D., Affatigato, M., Feller, S., Holland, D., Kemp, T. & Smith, M. *Phys. Chem. Glasses: Eur. J. Glass Sci. Technol. B*, 2012, **53**, 121.
3. Poplett, I. J. F. & Smith, M. E. *Solid State Nucl. Magn.*, **1998, 11**, 211.
4. Jellison, Jr., G. E., Feller, S. & Bray, P. J. *J. Magn. Reson.*, 1977, **27** 121.
5. Kemp, T. F. & Smith, M. E. *Solid State Nucl. Magn.*, 2009, **35**, 243. http://www2.warwick.ac.uk/fac/sci/physics/research/condensedmatt/nmr/research/calculations/quadfit/
6. Gaussian 03, Frisch, M. J., Trucks, G. W., Schlegel, H. B., Scuseria, G. E., Robb, M. A., Cheeseman, J. R., Montgomery, Jr., J. A., Vreven, T., Kudin, K. N., Burant, J. C., Millam, J. M., Iyengar, S. S., Tomasi, J., Barone, V., Mennucci, B., Cossi, M., Scalmani, G., Rega, N., Petersson, G. A., Nakatsuji, H., Hada, M., Ehara, M., Toyota, K., Fukuda, R., Hasegawa, J., Ishida, M., Nakajima, T., Honda, Y., Kitao, O., Nakai, H., Klene, M., Li, X., Knox, J. E., Hratchian, H. P., Cross, J. B., Adamo, C., Jaramillo, J., Gomperts, R., Stratmann, R. E., Yazyev, O., Austin, A. J., Cammi, R., Pomelli, C., Ochterski, J. W., Ayala, P. Y., Morokuma, K., Voth, G. A., Salvador, P., Dannenberg, J. J., Zakrzewski, V. G., Dapprich, S., Daniels, A. D., Strain, M. C., Farkas, O., Malick, D. K.,

Table 5. Asymmetry parameter from various trigonal borons

Asymmetry parameter	*Sample*	*Environment*	*Tetrahedral borons bonded per trigonal boron*
0·06	Crystalline lithium orthoborate, $3Li_2O.B_2O_3$	BO_3 triangles with 3 NBOs	0
0·12*	Boron oxide glass, B_2O_3	BO_3 triangles, all BOs with boroxol ring and non-ring borons and oxygens	0
0·16	Cesium enneaborate glass, $Cs_2O.9B_2O_3$	BO_3 triangles, all BOs with boroxol ring and triborate ring borons and oxygens	0 for boroxol rings 1 for triborate rings, net average 0·33
0·24	Cesium triborate glass, $Cs_2O.3B_2O_3$	BO_3 triangles, all BOs with triborate ring borons and oxygens	1
0·24	Cesium triborate crystal, $Cs_2O.3B_2O_3$	BO_3 triangles, all BOs with triborate ring borons and oxygens	1
0·25	Cesium diborate glass, $Cs_2O.2B_2O_3$	BO_3 triangles, all BOs with diborate ring borons and oxygens	2

*Average of three samples produced at cooling rates that varied over 10^8 K/s

Rabuck, A. D., Raghavachari, K., Foresman, J. B., Ortiz, J. V., Cui, Q., Baboul, A. G., Clifford, S., Cioslowski, J., Stefanov, B. B., Liu, G., Liashenko, A., Piskorz, P., Komaromi, I., Martin, R. L., Fox, D. J., Keith, T., Al-Laham, M. A., Peng, C. Y., Nanayakkara, A., Challacombe, M., Gill, P. M. W., Johnson, B., Chen, W., Wong, M. W., Gonzalez, C. & Pople, J. A. Gaussian, Inc., Wallingford CT, 2004.

7. Sinclair, R. N., Wright, A. C., Wanless, A. J., Hannon, A. C., Feller, S., Mayhew, M. T., Meyer, B. M., Royle, M. L., Wilkerson, D. L., Williams, R. B. & Johanson, B. C. In: *Borate Glasses, Crystals and Melts*, Eds. A. C. Wright, S. A. Feller & A. C. Hannon, The Society of Glass Technology, Sheffield, 1997, pp. 140.
8. Hannon, A. C., Grimley, D. I., Hulme, R. A., Wright, A. C. & Sinclair, R. N. *J. Non-Cryst. Solids*, 1994, **177**, 299.
9. Jellison, J. E., Panek, L. W., Bray, P. J. & Rouse, G. B. *J. Chem. Phys.*, 1977, **66**, 802.
10. Joo, C., Werner-Zwanziger, U. & Zwanziger, J. W. *J. Non-Cryst. Solids*, 2000, **261**, 282.
11. Joo, C., Werner-Zwanziger, U. & Zwanziger, J. W. *J. Non-Cryst. Solids*, 2000, **271**, 265.
12. Lee, S. K., Mibe, K., Fei, Y., Cody, G. D. & Mysen, B. O. *Phys. Rev. Lett.*, 2005, **94**, 165507.
13. Hwang, S.-J., Fernandez, C., Amoureux, J. P., Cho, J., Martin, S. W. & Pruski, M. *Solid State Nucl. Magn. Reson.*, 1997, **8**, 109.
14. Youngman, R. E. & Zwanziger, J. W. *J. Non-Cryst. Solids*, 1994, **168**, 293.
15. Gravina, S. J., Bray, P. J. & Petersen, G. L. *J. Non-Cryst. Solids*, 1990, **123**, 165.
16. Hung, I., Howes, A. P., Parkinson, B. G., Anup, T., Samoson, A., Brown, S. P., Harrison, P. F., Holland, D. & Dupree, R. *J. Solid State Chem.*, 2009, **182**, 2402.
17. Kroeker, S., Neuhoff, P. S. & Stebbins, J. F. *J. Non-Cryst. Solids*, 2001, **293–295**, 440.
18. Feller, S. A. PhD thesis, Brown University, 1980, p. 83.